CRYSTAL GROWTH & DESIGN

Article

pubs.acs.org/crystal

Host Polymorphs and Crystalline Host–Guest Complexes of 3,3′-Bis(9-hydroxy-9-fluorenyl)biphenyl

Konstantinos Skobridis,*[,†] Vassiliki Theodorou,*[,†] Wilhelm Seichter,[‡] and Edwin Weber*[,‡]

[†]Department of Chemistry, University of Ioannina, GR-451 10 Ioannina, Greece

[‡]Institut für Organische Chemie, Technische Universität Bergakademie Freiberg, Leipziger/Strasse 29, D-09596 Freiberg/Sachsen, Germany

Supporting Information

ABSTRACT: The diol host compound **2** featuring a structure with two 9-fluorenol moieties attached in 3,3′-position to a biphenyl core unit has been synthesized and is shown to form crystalline inclusion complexes with organic guest molecules. Aside from the single-crystal X-ray structures of unsolvated **2** in two polymorphous forms (**2A**, **2B**), structures of five inclusion compounds with 1,4-dioxane (**2a**), DMSO (**2b**), diethylamine (**2c**), acetic acid (**2d**), and ethyl acetate (**2e**) are described and comparatively discussed in the interaction behavior including corresponding host compounds with different attachment mode of the biphenyl unit and the diphenylhydroxymethyl-substituted equivalent.

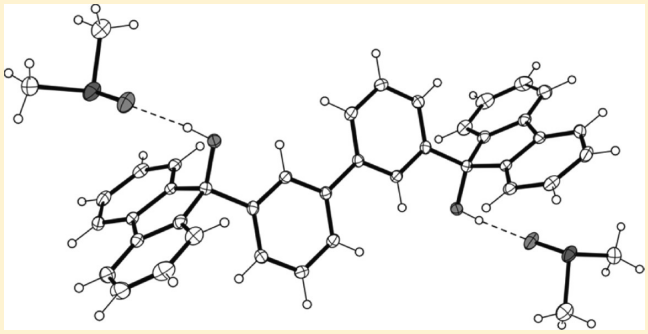

INTRODUCTION

Crystalline inclusion chemistry,[1−3] rated as an important subfield of crystal-engineering,[4−7] is a topic of actual interest in view of various scientific and practical aspects such as compound separation and storage.[8−11] Host molecules being endowed with this salient property have been developed by using specific design strategies that give rise to different types of host structures.[12−15] Among these, the bisfluorenol hosts show particular efficiency in the formation of crystalline inclusion compounds.[16] This is produced by the bulky fluorenol groups being attached to a rigid central unit mostly representing a biphenyl moiety. Numerous inclusion compounds of bisfluorenol hosts, such as **1** and **3** (Scheme 1), featuring 2,2′- and 4,4′-substitution of the biphenyl, respectively, have been isolated and studied via crystal structure analysis indicating specific behavior of guest inclusion depending on the substitution pattern.[16−22] Comparative investigation was also done involving closely related hosts where the terminal phenyl moieties are not covalently bonded as in the fluorene case, thus giving the phenyl rings an added degree of conformational freedom.[23] Moreover, host derivatives with elongated 2,2″-[1,1′:4′,1″]-terphenylene instead of 2,2′-biphenylene central moiety revealed another structural parameter to influence inclusion property.[24] However, inclusion formation of the 3,3′-substituted host analogue of the biphenylene bisfluorenol type, that is, **2** (Scheme 1), has neither been examined nor even synthesis of the host compound described to explore characteristics of inclusion behavior caused by this particular substitution pattern.

Here, we describe preparation of the host compound **2** and report crystal structures covering two polymorphs of the solvent free host (**2A**, **2B**) and five inclusion compounds of **2** (**2a**−**2e**)

Scheme 1. Compounds Studied in This Paper

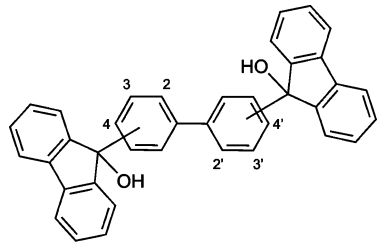

1 (2,2')
2 (3,3')
3 (4,4')

2A Polymorph-1
2B Polymorph-2

2a **2** · 1,4-Dioxane (1:3)
2b **2** · DMSO (1:2)
2c **2** · Diethylamine (1:2)
2d **2** · Acetic acid (2:1)
2e **2** · Ethyl acetate (1:1)

(Scheme 1) that involve guests of different functionality (proton donor and acceptor compounds of varied polarity). Furthermore, we make a comparison between the structures formed of the present host and known structures of positionally related host compounds or having freely rotating phenyl rings instead of

Received: May 7, 2013
Revised: June 24, 2013

   dx.doi.org/10.1021/cg400707s | *Cryst. Growth Des.* XXXX, XXX, XXX−XXX

Scheme 2. Synthesis of Host Compound 2

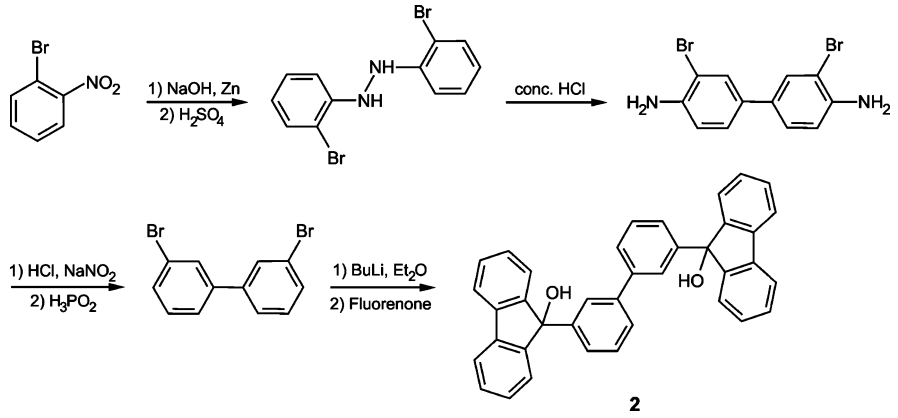

fluorene moieties showing potential behavior pattern created by the 3,3′-substitution mode.

RESULTS AND DISCUSSION

Host Synthesis. The host compound 3,3′-bis[9-hydroxy-9-fluorenyl]biphenyl (**2**) was synthesized by lithiation (*n*-BuLi/Et_2O) of 3,3′-dibromobiphenyl and subsequent reaction with 9-fluorenone. The starting compound 3,3′-dibromobiphenyl was prepared from *o*-nitrobromobenzene by reduction of the corresponding hydrazo compound, followed by rearrangement to the benzidine and deamination of the bis(diazonium) salt with hypophosphorous acid according to the literature procedure.[25] An illustration of the synthetic route is given in Scheme 2.

X-ray Structural Study. To elucidate the inclusion behavior of the new diol host **2**, a large number of crystallization experiments have been carried out using solvents of various classes of compounds with different polarity and proton donor/acceptor properties. Unfortunately, good quality crystals which could be structurally characterized by X-ray diffraction experiments were obtained only on a limited scale. Apart from two solvent-free crystals being polymorphs of **2** (**2A** and **2B**), they involve the inclusion compounds **2**·1,4-dioxane (1:3) (**2a**), **2**·DMSO (1:2) (**2b**), **2**·$HNEt_2$ (1:2) (**2c**), **2**·CH_3COOH (2:1) (**2d**), and **2**·$CH_3COOC_2H_5$ (1:1) (**2e**) (Scheme 1). ORTEP drawings of the molecular structures with the numbering of relevant atoms are presented in Figures 1 and 2, while the packing diagrams are shown in Figures 3−7. Crystallographic data, selected conformational parameters and information regarding hydrogen bond interactions in the crystals are listed in Tables 1−3. Because of the high content of aromatic building blocks, the conformation of the host molecule can be described by a set of dihedral angles between the plane fragments designated as A-D in the figures showing the molecular illustrations.

Crystallization of **2** from acetonitrile yields solvent-free crystals of the orthorhombic space group *Pbca* with the unit cell containing eight molecules, specified as polymorph **2A**. A perspective view of the molecular structure is illustrated in Figure 1a. On the other hand, crystal growing of **2** from chloroform or methacrylic acid resulted in a second unsolvated crystal structure of the polymorph **2B**, which has the monoclinic space group $P2_1/c$ with four molecules in the unit cell. In both of these polymorphs, the geometric features of the molecules are similar which is reflected by twist angles of 44.1(1) and 41.3(1)° between the rings of the biphenyl part and interplanar angles of 60.2(1) and 55.5(1)° formed by the pairs of the fluorenyl moieties, respectively (Table 2). The crystal structures are composed of O−H···O bonded molecular chains [O(2)−H(2)···O(1) 2.16 Å, 170°; 2.08 Å, 173°]. A packing excerpt of the orthorhombic form **2A** viewed down the crystallographic *c*-axis is depicted in Figure 3. Although the chain structures in the polymorphs **2A** and **2B** appear identical, the crystal structures reveal marked differences regarding the modes of interchain association (Table 3). In both cases, interconnection of the supramolecular strands occurs by the remaining OH hydrogens via O−H···π[26] interactions with fluorenyl units acting as acceptors [orthorhombic form O(1)−H(1)···C(30) 2.88 Å, 154°; monoclinic form O(1)−H(1)···C(31) 2.76 Å, 162°]. Intermolecular arene interactions of the C−H···π type[27] play a significant role in the orthorhombic polymorph **2A**, whereas the crystal structure of the monoclinic form **2B** is stabilized by edge-to-face arene interactions as well as face-to-face interactions[28,29] with a mean distance of 3.28 Å between interacting fluorenyl moieties (Figure 4). It should be noted at this point that according to Kitaigorodskii's close packing concept,[30] the more tightly packed polymorph of a compound can be regarded as the more stable one. Obviously, the observed packing indices of the present polymorphs are in accordance with this principle,[31] since the orthorhombic form **2A** has the higher packing coefficient (KPI 69.1), whereas the crystal lattice of the monoclinic polymorph **2B** (KPI 65.0) contains voids of 83.1 $Å^3$ per unit cell amounting to 4.4% of the unit cell volume.

The 1:3 inclusion compound of **2** with 1,4-dioxane (**2a**) crystallizes in the space group *P*-1 with one-half of the host molecule and one and a half molecules of solvent in the asymmetric part of the unit cell. The molecular structure is displayed in Figure 1b. According to inversion symmetry, the biphenyl unit of the host molecule is perfectly planar. The fluorenyl units adopt a slight distortion with a maximum atomic distance from the best plane being 0.089(1) Å for C(10) and −0.093 Å for C(13). The representative supramolecular entities of the crystal structure are given by O−H···O bonded 1:2 host−guest units [O(1)−H(1)···O(2A) 1.92 Å, 175°], which are further associated by the second oxygen of this guest molecule to form infinite strands [C(4)−H(4)···O(1A) 2.64 Å, 135°] (Figure 5). These hydrogen bonds lead to formation of 24-membered ring motifs of graph set R_4^6 [32,33] as integrated parts of the chain structure, each created by a pair of solvent molecules containing the acceptors (O atoms) and one fluorenol unit of two host molecules in each case containing the donors (OH and CH group). The remaining solvent molecules are located on

dx.doi.org/10.1021/cg400707s | Cryst. Growth Des. XXXX, XXX, XXX−XXX

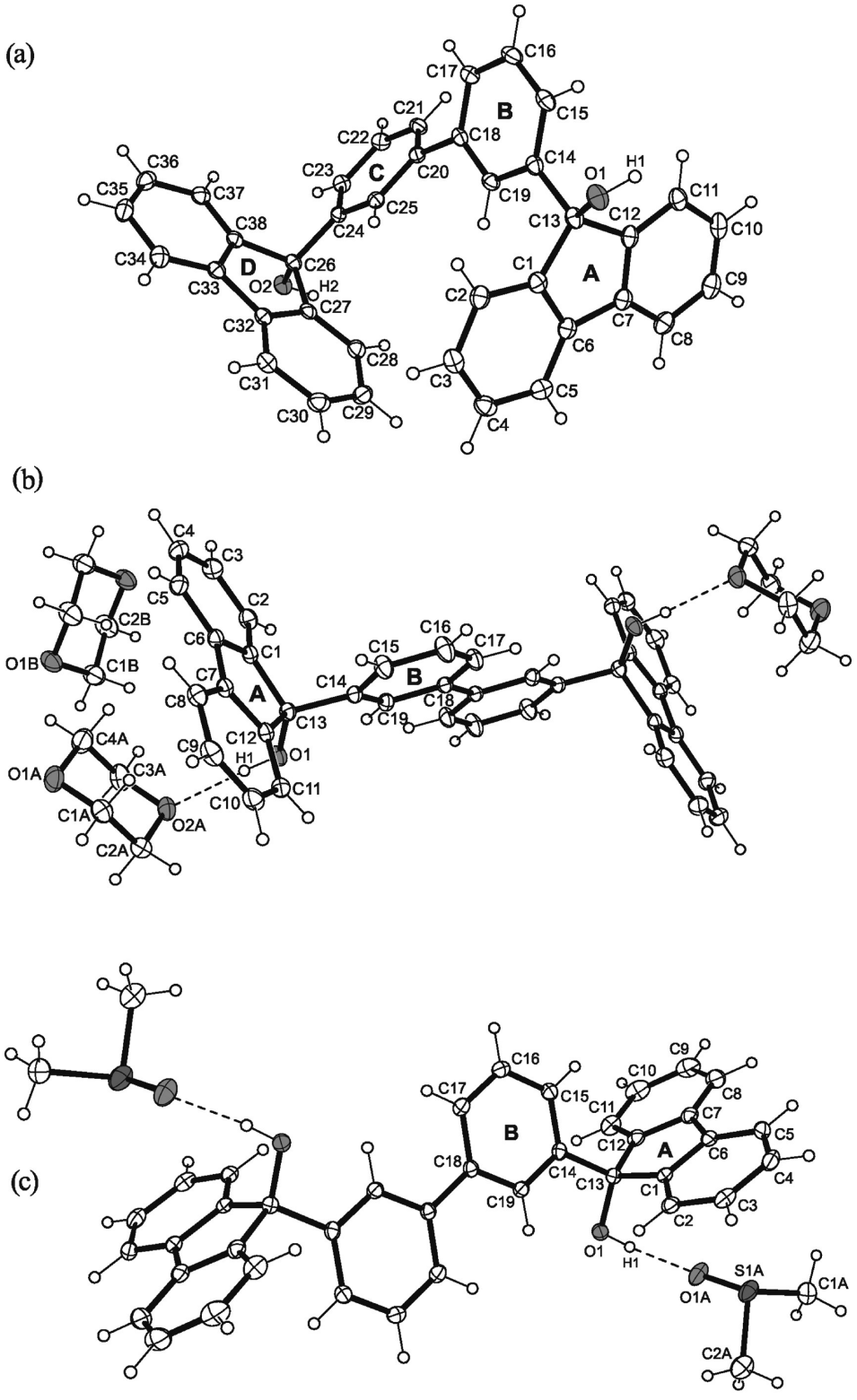

Fig. 1

Figure 1. ORTEP plots of the solvent-free structure **2** (orthorhombic form) (a), **2**·1,4-dioxane (1:3) (**2a**) (b), and **2**·DMSO (1:2) (**2b**) (c). Thermal ellipsoids are drawn at the 50% probability level. Broken lines represent hydrogen bond interactions.

interstitial places of the crystal lattice and are excluded from directed noncovalent bonding.

Crystallization of **2** from DMSO yields an 1:2 inclusion compound of the space group *P*-1 with one host molecule and

dx.doi.org/10.1021/cg400707s | *Cryst. Growth Des.* XXXX, XXX, XXX−XXX

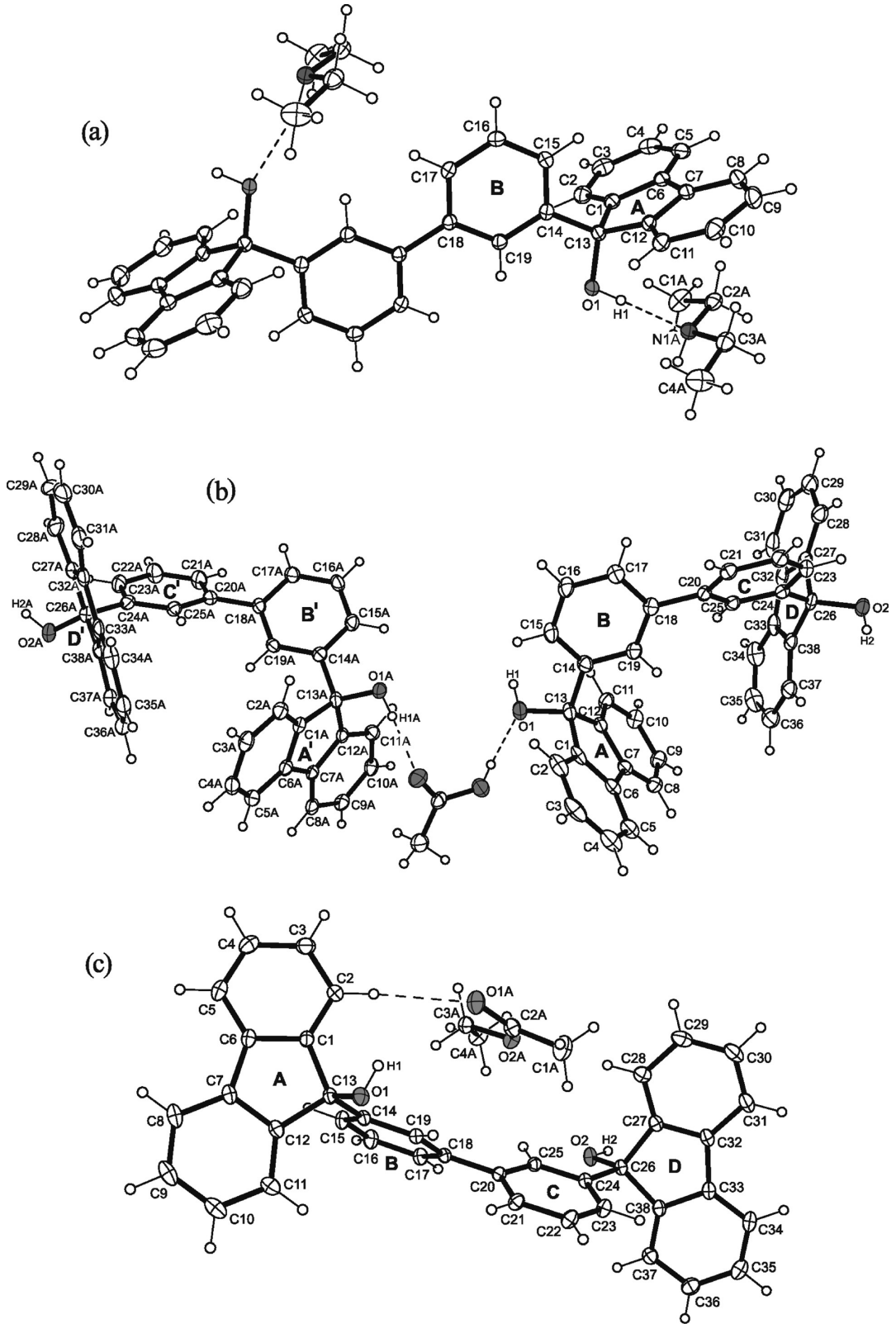

Figure 2. ORTEP diagrams of the inclusion structures **2**·diethylamine (1:2) (**2c**) (a), **2**·acetic acid (2:1) (**2d**) (b), and **2**·ethyl acetate (1:1) (**2e**) (c). Thermal ellipsoids are drawn at the 50% probability level. Broken lines represent hydrogen bond interactions.

two molecules of solvent in the unit cell. In a similar fashion as in the aforementioned case, the crystal structure of **2b** is composed of 1:2 host−guest units with the oxygen of the guest molecules hydrogen bonded to the hydroxy groups of the host [O(1)−H(1)···O(1A) 2.04 Å, 163°] (Figure 1c). Association of these complex units is accomplished by weak C−H···O interactions[26] with the hydroxy oxygens of the host [C(4)−H(4)···O(1) 2.62 Å, 141°] and the oxygen atom of the solvent molecule acting as acceptors [C(10)−H(10)···O(1A) 2.47 Å, 173°]. This bifurcated coordination mode of the solvent oxygen gives rise to

dx.doi.org/10.1021/cg400707s | *Cryst. Growth Des.* XXXX, XXX, XXX−XXX

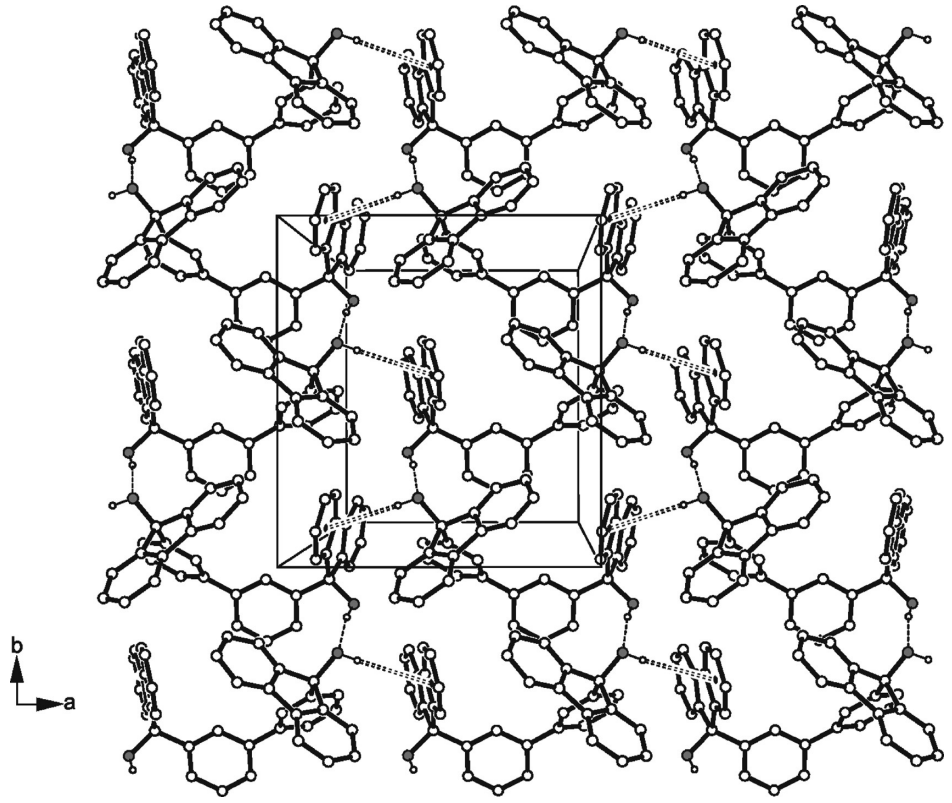

Figure 3. Packing excerpt of the solvent-free crystal structure of **2** (orthorhombic form) viewed down the crystallographic *c*-axis. Broken lines represent O−H···O hydrogen bonds, broken double lines O−H···π interactions.

formation of ring motifs of the graph set $R_4^2(16)$.[32,33] The crystal structure (Figure 6a) is constructed of infinite supramolecular strands running along the 111 direction. As the crystal lacks arene···arene contacts, interstrand interactions are reduced to van der Waals forces.

The 1:2 host−guest compound of **2** with diethylamine (**2c**) crystallizes in the monoclinic space group $P2_1/n$ with $Z = 2$, that is, the host molecule adopts inversion symmetry (Figure 2a). Because of the distinctive donor/acceptor ability of the crystal components, infinite strands of host and guest molecules are the basic supramolecular entities of the crystal structure. Within a given strand, the amino group of two solvent molecules and one OH group of two diol molecules create cyclic hydrogen bonded motifs of the graph set $R_4^4(8)$ [O(1)−H(1)···N(1A) 1.96 Å, 177°; N(1A)−H(1A)···O(1) 2.22(2) Å, 162(1) °]. As depicted in Figure 6b, molecules of adjacent chains are arranged nearly perpendicular to one another thus enabling intensive interstrand association via C−H···π interactions [d(H···π) = 2.69−2.86 Å].

The inclusion compound of **2** with acetic acid (2:1) (**2d**) crystallizes in the monoclinic space group $C2/c$ with the asymmetric part of the unit cell containing two crystallographically independent host molecules and one molecule of solvent (Figure 2b). The conformations of the host molecules basically differ from those found in the inclusion structures **2a**−**2c** but resemble those of the unsolvated crystal structures. The aromatic rings of the biphenyl element are twisted at angles of 42.3(1) and 39.0(1)°, the interplanar angles formed by the pairs of the fluorenyl units are 60.5(1) and 64.8(1)°, respectively. Because of packing and coordination effects, the fluorenyl moieties deviate to a more or less degree from planarity and show a marked distortion for the fluorenyl D′ with largest atomic distances from its mean plane being −0.105(2) and 0.086(2) Å for C(26A) and C(28A). The crystal structure of **2d** is characterized by extended tricyclic systems of hydrogen bonds (Figure 7a) each being composed of two symmetry related rings of the graph set $R_5^5(12)$, which comprise the hydroxy groups of four host molecules and the carboxyl group of one solvent molecule. The acetic acid also participates in a second supramolecular ring motif which is created by a C−H_{methyl}···O═C bonded dimer of carboxylic acid molecules following the graph set $R_2^2(8)$ [C(2B)-H(2B1)···O(1B) 2.54 Å, 164°]. As is evident from Table 3, a large number of C−H···π arene interactions [d(H···π)2.62−2.84 Å] complete the pattern of intermolecular interactions.

Crystallization of **2** from ethyl acetate yields colorless blocks of the monoclinic space group $C2/c$ ($Z = 8$) which turned out to be a 1:1 solvent complex **2e**, the structure of which is displayed in Figure 2c. The host molecule adopts an elongated geometry with a twist angle of 36.8(1)° between the aromatic rings of the biphenyl element and an interplanar angle of 31.5(1)° between the fluorenyl units. The carbonyl oxygen of the solvent molecule acts as a bifurcated acceptor, as it is coordinated to one of the hydroxy hydrogens of the host molecule [O(2)−H(2)···O(1A) 1.96 Å, 152°] and by a nonconventional hydrogen bond to an aryl hydrogen of a second host molecule [C(2)−H(2A)···O(1A) 2.54 Å, 166°]. The second hydroxy group of the host participates in host−host association [O(1)−H(1)···O(2) 2.04 Å, 163°]. In this way, the crystal structure of **2e** (Figure 7b) contains infinite molecular strands in which the molecules create cyclic hydrogen bonded motifs [graph set notation $R_3^2(9)$]. The supramolecular chains are interlinked by C−H···π type interactions.

Comparative Study of the Crystal Structures Including Isomeric and Related Hosts. As mentioned at the beginning, the main object of this study aims to identify distinctive features

dx.doi.org/10.1021/cg400707s | *Cryst. Growth Des.* XXXX, XXX, XXX−XXX

Table 1. Crystallographic and Structure Refinement Data of the Compounds Studied

	2A	2B	2a	2b	2c	2d	2e
empirical formula	$C_{38}H_{26}O_2$ polymorph 1	$C_{38}H_{26}O_2$ polymorph 2	$C_{38}H_{26}O_2{\cdot}3C_4H_8O_2$	$C_{38}H_{26}O_2{\cdot}2C_2H_6SO$	$C_{38}H_{26}O_2{\cdot}2C_4H_{11}N$	$C_{38}H_{26}O_2{\cdot}C_2H_4O_2$	$C_{38}H_{26}O_2{\cdot}C_4H_8O_2$
formula weight	514.59	514.59	778.90	670.84	660.86	1089.23	602.69
crystal system	orthorhombic	monoclinic	triclinic	triclinic	triclinic	monoclinic	monoclinic
space group	*Pbca*	$P2_1/c$	*P*-1	*P*-1	$P2_1/n$	$C2/c$	$C2/c$
a (Å)	11.2290(4)	18.5784(5)	8.3229(2)	8.2821(2)	11.8726(9)	40.6532(9)	47.2311(13)
b (Å)	12.1791(4)	11.3468(3)	8.4570(2)	8.3786(2)	13.1383(11)	12.2045(3)	9.0398(2)
c (Å)	38.4361(12)	12.3670(3)	15.3718(3)	13.5450(4)	12.2294(10)	22.8237(5)	14.5545(4)
α (deg)	90.0	90.0	95.525(1)	86.412(1)	90.0	90.0	90.0
β (deg)	90.0	96.731(1)	91.841(1)	72.722(1)	90.072(4)	94.682(4)	93.418(1)
γ (deg)	90.0	90.0	111.525(1)	73.155(1)	90.0	90.0	90.0
V (Å^3)	5256.5(3)	2589.06(12)	999.17(4)	858.71(4)	1907.6(3)	11286.2(4)	6203.1(3)
Z	8	4	1	1	2	8	8
$F(000)$	2160	1080	414	354	708	4576	2544
D_c (Mg m^{-3})	1.300	1.320	1.294	1.297	1.151	1.282	1.291
μ (mm^{-1})	0.079	0.080	0.087	0.198	0.070	0.080	0.082
data collection							
temperature (K)	100(2)	100(2)	100(2)	100(2)	100(2)	100(2)	100(2)
no. of collected reflections	44154	31850	21153	17009	33602	41032	51088
within the θ-limit (deg)	1.1−28.1	1.1−30.4	1.3−29.1	1.6−28.1	2.3−27.6	1.0−26.2	2.6−34.5
index ranges $\pm h$, $\pm k$, $\pm l$	−11/14, −11/16, −40/50	−26/24, −9/16, −17/17	−11/11, −11/11, −20/21	−10/10, −11/10, −17/17	−15/13, −17/17, −15/15	−50/50, −15/14, −28/28	−74/74, −14/14, −23/22
no. of unique reflections	6396	7818	5347	4172	4385	11270	13088
R_{int}	0.0281	0.0427	0.0263	0.0234	0.0290	0.0484	0.0326
refinement calculations: full-matrix least-squares on all F^2 values							
weighting expression w^a	$[\sigma^2(F_o^2)+(0.0446P)^2 + 2.7911P)^{-1}$	$[\sigma^2(F_o^2)+(0.0588P)^2 + 0.8696P)^{-1}$	$[\sigma^2(F_o^2)+(0.0593P)^2 + 0.2846P)^{-1}$	$[\sigma^2(F_o^2)+(0.0620P)^2 + 0.3259P)^{-1}$	$[\sigma^2(F_o^2)+(0.0476P)^2 + 0.6014P)^{-1}$	$[\sigma^2(F_o^2)+(0.0794P)^2 + 4.8707P)^{-1}$	$[\sigma^2(F_o^2)+(0.0700P)^2 + 2.4434P)^{-1}$
no. of refined parameters	363	363	263	220	233	763	419
no. of F values used $[I > 2\sigma(I)]$	5376	5714	4469	3620	3756	6836	10361
final R-indices							
R (=$\Sigma\lvert\Delta F\rvert/\Sigma\lvert F_o\rvert$)	0.0394	0.0467	0.0397	0.0358	0.0369	0.0549	0.0437
wR on F^2	0.1005	0.1238	0.1133	0.1127	0.0982	0.1591	0.1267
S (= goodness of fit on F^2)	1.017	1.013	1.046	1.075	1.021	1.023	1.023
final $\Delta\rho_{max}/\Delta\rho_{min}$ (e Å^{-3})	0.37/-0.22	0.41/-0.23	0.30/-0.24	0.39/-0.38	0.32/-0.21	0.31/-0.27	0.35/-0.21

$^aP = (F_o^2 + 2F_c^2)/3$.

dx.doi.org/10.1021/cg400707s | *Cryst. Growth Des.* XXXX, XXX, XXX−XXX

Table 2. Relevant Conformational Parameters of the Compounds Studied

	2A	2B	2a	2b	2c	2d	2e
			dihedral angles (deg)[a]				
mpla(A)−mpla(B)	80.5(1)	77.3(1)	83.1(1)	80.1(1)	84.8(1)	78.3(1)	87.8(1)
mpla(B)−mpla(C)	44.1(1)	41.3(1)				42.3(1)	36.8(1)
mpla(C)−mpla(D)	73.7(1)	76.1(1)				76.8(1)	82.5(1)
mpla(A)−mpla(D)	60.2(1)	55.5(1)				60.5(1)	31.5(1)
mpla(A′)−mpla(B′)						77.7(1)	
mpla(B′)−mpla(C′)						39.0(1)	
mpla(C′)−mpla(D′)						78.5(1)	
mpla(A′)−mpla(D′)						64.8(1)	
			torsion angles (deg)				
C(14)−C(13)−O(1)−H(1)	−88.0(1)	−90.8(1)	169.0(1)	−173.7(1)	172.2(1)	42.1(1)	90.9(1)
C(24)−C(26)−O(2)−H(2)	55.5(1)	54.9(1)				56.3(1)	−177.6(1)
C(14A)−C(13A)−O(1A)−H(1A)						−170.9(1)	
C(24A)−C(26A)−O(2A)−H(2A)						−112.3(1)	

[a]mpla means least-squares plane through the aromatic ring. Ring A: C(1)···C(13). Ring B: C(14)···C(19). Ring C: C(20)···C(25). Ring D: C(26)···C(38). Ring A′: C(1A)···C(13A). Ring B′: C(14A)···C(19A). Ring C′: C(20A)···C(25A). Ring D′: C(26A)···C(38A).

of the solid state structures of the host compound **2** providing the basis for a detailed comparison with the known crystal structures formed of the constitutionally isomeric 2,2′- and 4,4′-difluorenol-substituted biphenyl derivatives **1**[16−19,34,35] and **3**,[20−22,36,37] respectively, and making a further comparison with the related diphenylhydroxymethyl analogous host compound possible.[23]

With reference to the structures of the unsolvated species, the following distinctions can be made. Depending on whether acetonitrile or chloroform was used as a solvent for crystal growing, **2** was found to exist in an orthorhombic or monoclinic crystal structure. In both cases, the molecules adopt a compact twisted geometry which appears to be controlled by close packing requirements rather than noncovalent bonding. The crystal structures of the polymorphs are composed of the same kind of O−H···O bonded strands which, however, show different modes of interchain association comprising O−H···π and arene−arene interactions. A similar compact molecular geometry is also observed in the crystal structure of the unsolvated 2,2′-disubstituted biphenyl derivative **1**.[35] But unlike **2**, the molecular geometry of this latter isomer is determined by a strong intramolecular hydrogen bond between the hydroxy groups, which induces a helical conformation with a nearly orthogonal twist of the biphenyl unit. The hydroxy hydrogen, not involved in O−H···O bonding, is engaged in a relatively strong intermolecular O−H···π arene contact thus creating a supramolecular dimer as the basic structure entity. Finally, the 4,4′-disubstituted biphenyl isomer **3** adopts an elongated conformation, which prevents formation of intramolecular hydrogen bonding. In the solvent-free state, the hydroxy groups of the molecule lack any directed noncovalent bonding, so that the crystal structure seems to be stabilized only by van der Waals forces.[18]

The present host molecule **2** made it possible for us to isolate and structurally study single crystals of the inclusion compounds **2a**−**2e** involving guests of different shape and polarity. As a matter of principle, their crystal structures suggest considerable conformational flexibility for the host molecule. In presence of a highly cross-linking solvent species, as in the inclusion structure of **2** with acetic acid (**2d**), the host molecule adopts a strongly twisted conformation with a close distance of the fluorenyl units. On the other side, in cases where the host adopts inversion symmetry (**2a**−**2c**), as well as in the solvent inclusion of **2** with ethyl acetate (**2e**), the molecule exists in an undistorted elongated conformation with the hydroxy groups pointing away from the molecular backbone resulting in a chain-like aggregation of molecules.

Unlike **2**, in the inclusion structures of the 2,2′-disubstituted host isomer **1**, the molecular geometry is locked by a strong intramolecular O−H···O hydrogen bond which enforces a helical conformation. As a consequence, only one strong donor and acceptor site is available for molecular association. This may explain why formation of discrete host guest aggregates are favored over three-dimensional molecular association via hydrogen bonding. Nevertheless, this host compound has proven to be very efficient in formation of crystalline inclusions with a broad variety of organic guest solvents of different nature[16−18,34,35] including oligofunctional and conjugate functional group containing species.[19]

In the inclusion structures of the 4,4′-disubstituted host isomer **3**,[20−22,36,37] the host molecule adopts an elongated geometry irrespective of some degree of conformational freedom. This relatively rigid molecular geometry may explain the strong tendency of this host to create a channel-like cavity structure with guest-specific dimensions.

Another interesting way to elucidate structural relationships is to compare the crystal structures of the bisfluorenol host **2** with those formed of the known diphenylhydroxymethyl substituted analogue, that is, having separate phenyl substituents instead of linked ones in the fluorene moiety.[23] The solvent-free crystal structure of the respective host lacks molecular association via conventional hydrogen bonding, which may be ascribed to an enhanced shielding effect caused by the distorted terminal phenyl rings. On the contrary, the OH groups participate in formation of weaker O−H···π interactions, which interlink the molecules to a three-dimensional network. Only a small number of inclusion structures of this host system have been characterized, comprising acetone, 2-cyclopenten-1-one, and acetic acid as guest component.[23] Similar to the inclusion structures of **2**, the crystals of this particular host inclusions are constructed of infinite hydrogen bonded strands, which, however, differ in their patterns of host−guest aggregation. In the 1:1 host−guest complex with acetic acid, the guest molecules create the well-known O−H···O bonded dimers,[38] which are further linked with host molecules to form infinite strands. On the other side, crystal growing of **2** from acetic acid yields a 2:1 complex (**2d**), which is characterized by a complicated tricyclic system of hydrogen

dx.doi.org/10.1021/cg400707s | Cryst. Growth Des. XXXX, XXX, XXX−XXX

Table 3. Noncovalent Interactions in the Crystal Structures Studied

atoms involved D−H···A	symmetry operator	distance D···A	distance H···A	angle D−H···A
	2A			
O(1)−H(1)···C(30)[b]	1 + *x*, *y*, *z*	3.660(1)	2.88	154
O(2)−H(2)···O(1)	0.5 − *x*, −0.5 + *y*, *z*	2.987(1)	2.16	170
C(15)−H(15)···O(1)	*x*, *y*, *z*	2.831(1)	2.51	100
C(9)−H(9)···*cg*(ring A1)[a]	1 − *x*, −0.5 + *y*, 0.5 − *z*	3.555(2)	2.63	164
C(5)−H(5)···C(10)[b]	−0.5 + *x*, *y*, 0.5 − *z*	3.729(2)	2.90	147
C(2)-H(2A)···*cg*(ring C)[a]	0.5 − *x*, 0.5 + *y*, *z*	3.534(2)	2.63	159
C(16)−H(16)···*cg*(ring D2)[a]	1 + *x*, *y*, *z*	3.584(2)	2.74	148
	2B			
O(1)−H(1)···C(31)[b]	*x*, −1 + *y*, *z*	3.469(2)	2.76	162
O(2)−H(2)···O(1)	*x*, 1.5 − *y*, 0.5+*z*	2.913(1)	2.08	173
C(23)−H(23)···O(2)	*x*, *y*, *z*	2.790(2)	2.47	100
C(2)-H(2A)···C(28)[b]	*x*, −1 + *y*, *z*	3.600(2)	2.88	133
C(11)−H(11)···*cg*(ring C)[a]	*x*, 1.5 − *y*, −0.5 + *z*	3.535(2)	2.59	171
C(15)−H(15)···C(33)[b]	*x*, −1 + *y*, *z*	3.534(2)	2.73	143
C(23)−H(23)···C(15)[b]	*x*, 1.5 − *y*, 0.5 + *z*	3.436(2)	2.85	121
C(30)−H(30)···C(3)[b]	*x*, 1.5 − *y*, 0.5 + *z*	3.563(2)	2.73	147
C(35)−H(35)···*cg*(ring C)[a]	−*x*, 2 − *y*, 1 − *z*	3.534(2)	2.75	141
	2a			
O(1)−H(1)···O(2A)	1 + *x*, 1 + *y*, *z*	2.759(1)	1.92	175
C(19)−H(19)···O(1)	*x*, *y*, *z*	2.710(1)	2.38	101
C(2)−H(2)···C(9)[b]	−1 + *x*, *y*, *z*	3.652(1)	2.88	139
C(4)−H(4)···O(1A)	1 − *x*, 1 − *y*, −*z*	3.377(1)	2.64	135
C(9)−H(9)···O(1)	1 + *x*, *y*, *z*	3.465(1)	2.66	143
C(10)−H(10)···C(17)[b]	1 + *x*, 1 + *y*, *z*	3.561(1)	2.85	132
C(17)−H(17)···C(10)[b]	2 − *x*, 1 − *y*, 1 − *z*	3.723(1)	2.85	154
	2b			
O(1)−H(1)···O(1A)	*x*, *y*, *z*	2.851(1)	2.04	163
C(10)−H(10)···O(1A)	−*x*, 1 − *y*, −*z*	3.415(2)	2.47	173
C(4)−H(4)···O(1)	1 + *x*, *y*, *z*	3.413(2)	2.62	141
C(19)−H(19)···O(1)	*x*, *y*, *z*	2.740(2)	2.40	100
	2c			
O(1)−H(1)···N(1A)	1 + *x*, *y*, *z*	2.803(1)	1.96	177
N(1A)−H(1A)···O(1)	1 − *x*, −*y*, 1 − *z*	3.082(1)	2.22(2)	162(1)
C(19)−H(19)···O(1)	*x*, *y*, *z*	2.711(1)	2.34	103
C(5)−H(5)···*cg*(ring B)[a]	1.5 − *x*, 0.5 + *y*, 0.5 − *z*	3.542(2)	2.72	145
C(3A)−H(3A2)···*cg*(ring A2)[a]	−1 + *x*, *y*, *z*	3.576(2)	2.70	148
C(8)−H(8)···C(18)[b]	0.5 + *x*, 0.5 − *y*, −0.5 + *z*	3.554(1)	2.69	152
C(11)−H(11)···C(4)[b]	1.5 − *x*, −0.5 + *y*, 0.5 − *z*	3.387(1)	2.86	116
	2d			
O(1)−H(1)···O(2A)	*x*, −*y*, −0.5 + *z*	2.853(2)	2.03	167
O(2A)−H(2A1)···O(2)	*x*, *y*, 1 + *z*	2.860(2)	2.21	135
O(1A)−H(1A)···O(1B)	*x*, *y*, *z*	2.736(2)	1.90	174
O(2)−H(2)···O(1A)	*x*, 1 − *y*, −0.5 + *z*	2.761(2)	1.93	173
O(2B)−H(2B)···O(1)	*x*, 1 + *y*, *z*	2.700(2)	1.87	172
C(2B)−H(2B1)···O(1B)	0.5 − *x*, 1.5 − *y*, 1 − *z*	3.490(2)	2.54	164
C(23)−H(23)···O(2)	*x*, *y*, *z*	2.793(2)	2.47	100
C(9)−H(9)···C(5)[b]	0.5 − *x*, 0.5 + *y*, 0.5 − *z*	3.641(3)	2.85	142
C(16)−H(16)···C(32)[b]	*x*, −*y*, 0.5 + *z*	3.589(3)	2.83	138
C(23)−H(23)···C(15A)[b]	*x*, 1 − *y*, −0.5 + *z*	3.446(3)	2.82	124
C(30)−H(30)···C(22)[b]	−*x*, −*y*, −*z*	3.705(3)	2.79	162
C(35)−H(35)···C(10A)[b]	*x*, −*y*, −0.5 + *z*	3.700(3)	2.82	154
C(2)−H(2A)···*cg*(ring C)[a]	*x*, −*y*, −0.5 + *z*	3.489(3)	2.62	153
C(11A)−H(11A)···*cg*(ring D2′)[a]	*x*, 1 − *y*, −0.5 + *z*	3.627(3)	2.78	148
C(16A)−H(16A)···*cg*(ring D1′)[a]	*x*, 1 − *y*, −0.5 + *z*	3.508(3)	2.62	152
C(5A)−H(5A)···*cg*(ring A2)[a]	0.5 − *x*, 0.5 − *y*, 1 − *z*	3.681(3)	2.80	154
C(2A)−H(2A2)···*cg*(ring C)[a]	*x*, 1 − *y*, 0.5 + *z*	3.551(3)	2.63	163
C(16)−H(16)···*cg*(ring D1)[a]	*x*, 1 − *y*, 0.5 + *z*	3.767(3)	2.84	165
C(29A)−H(29A)···C(25A)[b]	*x*, −*y*, 0.5 + *z*	3.780(3)	2.84	162

dx.doi.org/10.1021/cg400707s | *Cryst. Growth Des.* XXXX, XXX, XXX−XXX

Table 3. continued

atoms involved D−H···A	symmetry operator	distance D···A	distance H···A	angle D−H···A
2e				
O(1)−H(1)···O(2)	1 + *x*, *y*, *z*	2.851(1)	2.04	163
O(2)−H(2)···O(1A)	*x*, 1 + *y*, *z*	2.730(1)	1.96	152
C(2)−H(2A)···O(1A)	*x*, *y*, *z*	3.474(1)	2.54	166
C(19)−H(19)···O(1)	*x*, *y*, *z*	2.761(1)	2.39	103
C(25)−H(25)···O(2)	*x*, *y*, *z*	2.689(1)	2.33	101
C(3)−H(3)···C(18)[b]	*x*, −*y*, −0.5 + *z*	3.685(1)	2.74	174
C(4)−H(4)···C(9)[b]	*x*, −1 − *y*, 0.5 + *z*	3.672(1)	2.86	144

[a]Means center of the aromatic ring. Ring A1: C(1)···C(6). Ring A2: C(7)···C(12). Ring B: C(14)···C(19). Ring C: C(20)···C(25). Ring D1: C(27)···C(32). Ring D2: C(33)···C(38). Ring D1′: C(27A)···C(32A). Ring D2′: C(33A)···C(38A). [b]To achieve a reasonable hydrogen bond geometry, an individual atom instead the ring centroid was chosen as acceptor.

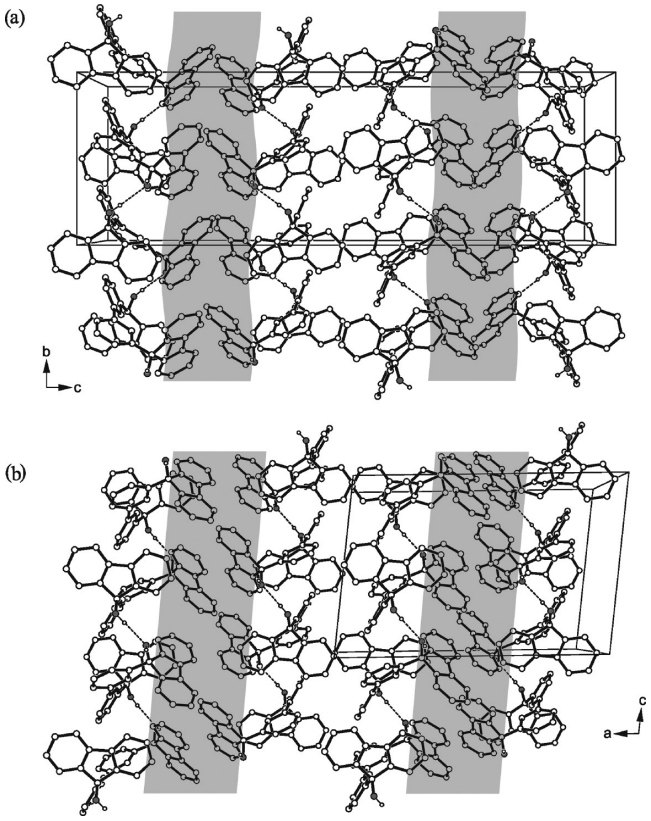

Figure 4. Packing excerpts of the polymorphic structures of **2**. (a) Orthorhombic polymorph **2A** viewed down the *a*-axis. Structure domains marked by shading represent arene edge-to-face interactions. (b) Monoclinic polymorph **2B** viewed down the *b*-axis. Structure domains marked by shading represent arene face-to-face interactions. Broken lines represent O−H···O hydrogen bonds.

bonds. In this remarkable coordination pattern, a pair of C−H···O═C bonded solvent molecules represent the central ring. The carboxylic groups of these molecules also take part in the formation of two more extended O−H···O bonded ring systems each being formed by the OH groups of four different host molecules.

CONCLUSION

A new bulky diol compound **2** featuring a structure with two 9-fluorenol moieties positionally 3,3′-attached to a central biphenyl unit that fills the gap between the known 2,2′- and 4,4′-substituted analogues, that is, **1** and **3**, has been synthesized and is shown to behave as host molecule for crystalline inclusion formation similar, in principle, to **1** and **3**. This is demonstrated by the inclusion compounds **2a**−**2e** involving guests of different shape and functionality, which have been isolated and structurally studied. Nevertheless, guest free crystals could also be obtained in two polymorphous forms (**2A**, **2B**) when crystallized from acetonitrile or chloroform showing that solvent inclusion may not to happen under particular conditions. A main statement, however, is deduced from a comparative inspection comprising the presently studied and the known structures of the 2,2′- and 4,4′-disubstituted host isomers, which clearly illustrates how the connection mode of the biphenyl element, either 2,2′-, 3,3′-, or 4,4′-, distinctly exercises an influence on the inclusion behavior by implication of changed molecular flexibility and supramolecular interactions including availability of the host functional groups for the complex formation. From this point of view, the host compound **2** is closer to **3** than to **1**. This is attributed to the high conformational rigidity in **1** because of the strong intramolecular hydrogen bond between the hydroxyls leading to strict mono proton donor and acceptor nature in the host−guest interaction with reference to the coordinating groups. By way of contrast, **2** and **3** are not restrained in this respect giving rise to conformational flexibility and supporting bifunctionality of the molecules. Thus, although the host compounds of the given series **1**-**3** are composed of the same building units, but in different connection, show rather distinctive host character.

EXPERIMENTAL SECTION

General. The melting point (uncorrected) was determined with a Reichert hot stage apparatus. The IR spectrum (cm^{-1}) was recorded with a Perkin-Elmer FT-IR 1600 spectrometer. ^{1}H and ^{13}C NMR spectra were measured for solutions (Me_4Si as internal standard, ppm) with a Bruker AMX 250 MHz spectrometer. The high resolution ESI mass spectrum was obtained using a ThermoFisher Scientific Orbitrap XL spectrometer.

Reactions were monitored by thin-layer chromatography carried out on Merck silica gel 60 F_{254}-coated plates. For column chromatography, silica gel (Merck, particle size 0.040−0.063 mm, 230−240 mesh) was used. All reagents were commercial products and were used without further purification. The solvents used were purified or dried by standard procedures.[39] The starting compounds 2-nitrobromobenzene and fluoren-9-one were purchased from Janssen. 3,3′-Dibromobiphenyl was prepared according to the literature procedure.[25]

Synthesis of 3,3′-Bis(9-hydroxy-9-fluorenyl)biphenyl (2). A solution of *n*-BuLi (1.6 M in *n*-hexane, 12.5 mL, 20 mmol) was added dropwise at −78 °C under argon and under stirring to 3,3′-dibromobiphenyl (3.10 g, 10 mmol) dissolved in dry diethyl ether (40 mL). Stirring of the mixture was continued at −20 °C for 10 min. Then,

dx.doi.org/10.1021/cg400707s | *Cryst. Growth Des.* XXXX, XXX, XXX−XXX

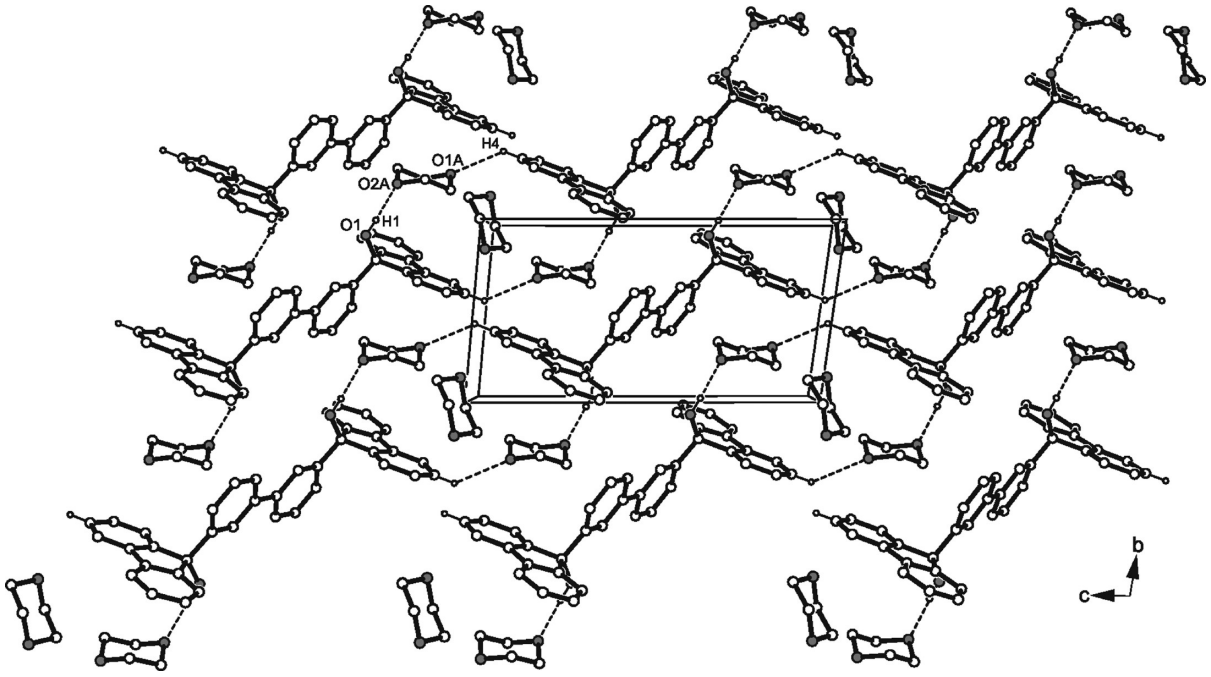

Figure 5. Packing excerpt of the inclusion structure **2**·1,4-dioxane (1:2) (**2a**) viewed down the crystallographic *a*-axis. Broken lines represent hydrogen bond type interactions.

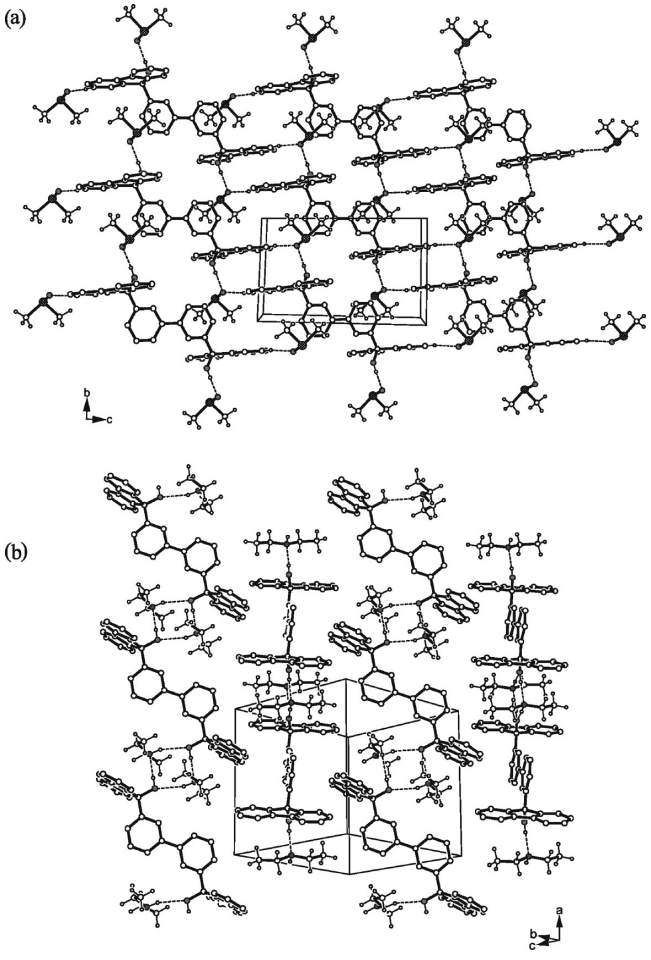

Figure 6. Packing diagrams of the inclusion structures **2**·DMSO (1:2) (**2b**) (a) and **2**·diethylamine (1:2) (**2c**) (b). Broken lines represent hydrogen bond interactions.

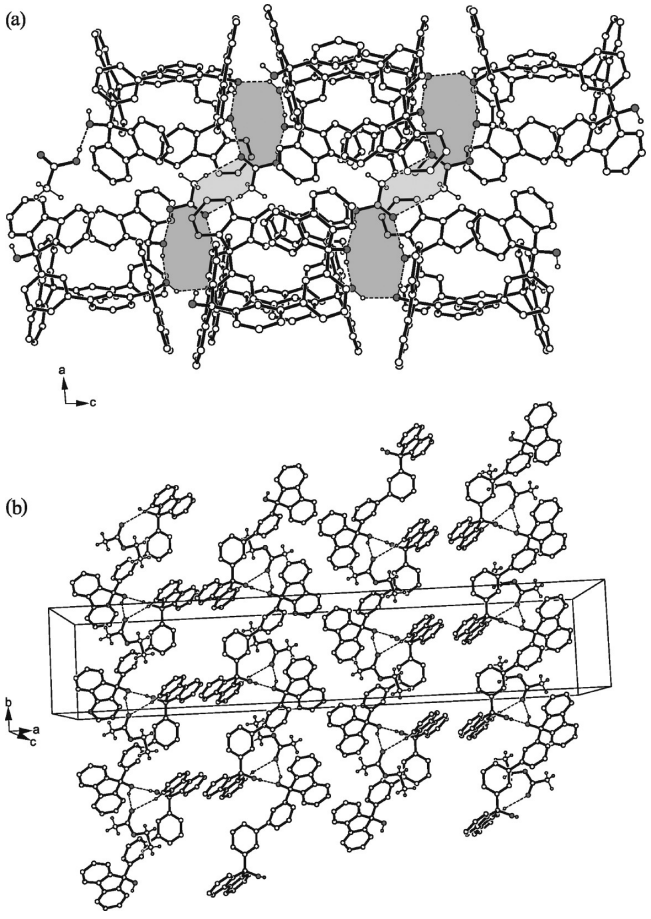

Figure 7. Packing diagrams of the inclusion structures **2**·acetic acid (2:1) (**2d**) (a) and **2**·ethyl acetate (1:1) (**2e**) (b). Broken lines represent hydrogen bond interactions.

dx.doi.org/10.1021/cg400707s | *Cryst. Growth Des.* XXXX, XXX, XXX−XXX

fluorenone (3.78 g, 21 mmol) in dry diethyl ether (40 mL) was added and the mixture was kept at reflux. After completion of the reaction (20 h), which was monitored by TLC (hexane/ethyl acetate 2:1), the reaction mixture was cooled, quenched with saturated aqueous NH_4Cl solution and extracted with Et_2O (2 × 30 mL). The combined organic extracts were dried (Na_2SO_4) and evaporated. Recrystallization from ethyl acetate yielded a first crop (2.20 g, 43%) of pure product. A second crop (1.14 g, 22%) was obtained from the filtrate, which was evaporated and purified by flash chromatography on SiO_2 column (hexane/ethyl acetate 2:1). Total yield 65% of colorless solid; mp 219−221 °C. IR (KBr) ν 3035 (OH), 3035 (C−H, arom.), 1599 (C═C), 1446, 1282, 1035; ^{1}H NMR (250 MHz, $CDCl_3$) δ 2.56 (s, br, OH, 2H), 7.28−7.50 (m, 18H, ArH), 7.73−7.79 (m, 6H, ArH); ^{13}C NMR (63 MHz, $CDCl_3$) δ 83.8 (CO), 120.3, 124.4, 124.6, 124.9, 126.4, 128.6, 129.3, 139.7, 141.4, 143.8, 150.4 (Ar). MS (ESI) m/z calcd for $[C_{38}H_{26}O_2 + Na]^+$: 537.6120; found $[M + Na]^+$ 537.1825.

X-ray Crystallography. Crystals of the polymorphs **2A** and **2B** suitable for X-ray diffraction were obtained by slow crystallization of **2** from acetonitrile and chloroform, respectively. Suitable crystals of the inclusion compounds **2a**−**2e** were grown by slow evaporation of solutions of **2** in the respective solvent. The intensity data were collected on a Bruker APEX II diffractometer with MoK_α radiation (λ = 0.71073 Å) using ω- and ϕ-scans. Reflections were corrected for background, Lorentz and polarization effects. Preliminary structure models were derived by application of direct methods[40] and were refined by full-matrix least-squares calculation based on F^2 for all reflections.[41] The non-hydrogen atoms were refined with anisotropic thermal parameters. With the exception of the amino hydrogen H(1A) in the structure of **2c**, all other hydrogen atoms were included in the models in calculated positions and were refined as constrained to bonding atoms.

■ ASSOCIATED CONTENT

Ⓢ Supporting Information

X-ray crystallographic data in CIF format for the structures reported in this paper. This material is available free of charge via the Internet at http://pubs.acs.org.

■ AUTHOR INFORMATION

Corresponding Author

*E-mail: kskobrid@cc.uoi.gr (K.S.); Edwin.Weber@chemie.tu-freiberg.de (E.W.).

Notes

The authors declare no competing financial interest.

■ REFERENCES

(1) Atwood, J. L.; Davies, J. E. D.; MacNicol, D. D. *Inclusion Compounds*; Oxford University Press: Oxford, U.K., 1991; Vol. *4*.
(2) Weber, E. *Molecular Inclusion and Molecular Recognition-Clathrates I and II*; Topics in Current Chemistry; Springer-Verlag: Berlin, 1987 and 1988; Vols. *140* and *149*.
(3) Herbstein, F. H. *Crystalline Molecular Complexes and Compounds*; IUCR Monographs on Crystallography; Oxford University Press: Oxford, U.K., 2005; Vol. *1*.
(4) Desiraju, G. R. *Crystal Engineering*; Materials Science Monographs; Elsevier: Amsterdam, 1989; Vol. *54*, pp 175−198.
(5) Weber, E. *Design of Organic Solids*; Topics in Current Chemistry; Springer-Verlag: Berlin, 1998; Vol. *198*.
(6) *Making Crystals by Design: Methods, Techniques and Applications*; Braga, D., Creponi, F., Eds.; Wiley-VCH: Weinheim, Germany, 2007.
(7) *Organic Crystal Engineering*; Tiekink, E. R. T., Vittal, J. J. Zaworotko, M. J., Eds.; Wiley: Chichester, U.K., 2010.
(8) *Comprehensive Supramolecular Chemistry*; MacNicol, D. D., Toda, F., Bishop, R., Eds.; Elsevier: Oxford, U.K., 1996; Vol. *6*.
(9) Hertzsch, T.; Hulliger, J.; Weber, E.; Sozzani, P. In *Encyclopedia of Supramolecular Chemistry*; Atwood, J. L., Steed, J. W., Eds.; CRC Press: Boca Raton, FL, U.S.A., 2004; pp 996−1005.
(10) *Organic Solid State Reactions, Topics in Current Chemistry*; Toda, F., Ed.; Springer-Verlag: Berlin, 2005; Vol. *254*.
(11) *Metal−Organic Frameworks: Design and Application*; Gillivray, L. R., Ed.; Wiley: Hoboken, NJ, U.S.A., 2010.
(12) Weber, E. In *Inclusion Compounds*; Atwwod, J. L., Davies, J. E. D., MacNicol, D. D., Eds.; Oxford University Press: Oxford, U.K., 1991; Vol. *4*, pp 188−262.
(13) Bishop, R. *Chem. Soc. Rev.* **1996**, *25*, 311−319.
(14) Desiraju, G. R. In *Comprehensive Supramolecular Chemistry*; MacNicol, D. D., Toda, F., Bishop, R., Eds.; Elsevier: Oxford, U.K., 1996; Vol. *6*, pp 1−22.
(15) Nangia, A. In *Nanoporous Materials*; Series on Chemical Engineering; Lu, G. Q., Zhao, X. S., Eds.; Imperial College Press: London, 2004; Vol. *4*, pp 165−187.
(16) Weber, E. In *Comprehensive Supramolecular Chemistry*; MacNicol, D. D., Toda, F., Bishop, R., Eds.; Elsevier: Oxford, U.K., 1996; Vol. *6*, pp 535−592.
(17) Weber, E.; Skobridis, K.; Wierig, A.; Stathi, S.; Nassimbeni, L. R.; Niven, M. L. *Angew. Chem., Int. Ed. Engl.* **1993**, *32*, 606−608.
(18) Caira, M. R.; Le Roex, T.; Nassimbeni, L. R.; Ripmeester, J. A.; Weber, E. *Org. Biomol. Chem.* **2004**, *2*, 2299−2304.
(19) Skobridis, K.; Theodorou, V.; Alivertis, D.; Seichter, W.; Weber, E.; Csöregh, I. *Supramol. Chem.* **2007**, *19*, 373−382.
(20) Weber, E.; Nitsche, S.; Wierig, A.; Csöregh, I. *Eur. J. Org. Chem.* **2002**, 856−872.
(21) Le Roex, T.; Nassimbeni, L. R.; Weber, E. *Chem. Commun.* **2007**, 1124−1126.
(22) Bourne, S. A.; Corin, K.; Cruickshank, D. L.; Davson, J.; Nassimbeni, L. R.; Su, H.; Weber, E. *New J. Chem.* **2011**, *35*, 1556−1561.
(23) Skobridis, K.; Paraskevopoulos, G.; Theodorou, V.; Seichter, W.; Weber, E. *Cryst. Growth Des.* **2011**, *11*, 5275−5288.
(24) Klien, H.; Seichter, W.; Weber, E. *CrystEngComm* **2013**, *15*, 586−596.
(25) Snyder, H. R.; Weaver, C.; Marshall, C. D. *J. Am. Chem. Soc.* **1949**, *71*, 289−291.
(26) Desiraju, G. R.; Steiner, T. *The Weak Hydrogen Bond*; Oxford University Press: Oxford, U.K., 1999; pp 29−121.
(27) Nishio, M.; Umezawa, Y.; Honda, K.; Tsuboyama, S.; Suezawa, H. *CrystEngComm* **2009**, *11*, 1757−1788.
(28) Dance, I. In *Encyclopedia of Supramolecular Chemistry*; Atwood, J. L., Steed, J. M., Eds.; Dekker: New York, 2004; pp 1076−1092.
(29) Salonen, L. M.; Ettermann, M.; Diederich, F. *Angew. Chem., Int. Ed.* **2011**, *50*, 4808−4842.
(30) Kitaigorodskii, A. I. In *Organic Chemical Crystallography*; Consultant Bureau: New York, 1961; Ch. 3.
(31) *PLATON*, version 1.15; University of Glasgow: Glasgow, U.K., 2008.
(32) Etter, M. C. *J. Phys. Chem.* **1991**, *95*, 4601−4610.
(33) Bernstein, J.; Davies, R. E.; Shimoni, L.; Chang, N.-L. *Angew. Chem., Int. Ed.* **1995**, *34*, 1555−1573.
(34) Barbour, L. J.; Bourne, S. A.; Caira, M. R.; Nassimbeni, L. R.; Weber, E.; Skobridis, K.; Wierig, A. *Supramol. Chem.* **1993**, *1*, 331−336.
(35) Skobridis, K.; Theodorou, V.; Seichter, W.; Weber, E. *Cryst. Growth Des.* **2010**, *10*, 862−869.
(36) Caira, M. R..; Le Roex, T.; Nassimbeni, L. R.; Weber, E. *Cryst. Growth Des.* **2006**, *6*, 127−131.
(37) Le Roex, T.; Nassimbeni, L. R.; Weber, E. *New. J. Chem.* **2008**, *32*, 856−863.
(38) Jeffrey, G. A. *An Introduction to Hydrogen Bonding*; Oxford University Press: Oxford, U.K., 1997.
(39) Leonhard, J.; Lygo, B.; Procter, G. *Praxis der Organischen Chemie*; VCH-Verlagsgesellschaft: Weinheim, Germany, 1996; pp 53−68.
(40) Sheldrick, G. M. *SHELXS-97: Program for Crystal Structure Solution*; University of Göttingen: Göttingen, Germany, 1997.
(41) Sheldrick, G. M. *SHELXL-97: Program for Crystal Structure Refinement*; University of Göttingen: Göttingen, Germany, 1997.